Inhibition of SND1 overcomes chemoresistance in bladder cancer cells by promoting ferroptosis

YU ZHAO, PENGPENG REN, ZHIQIN YANG, LEI WANG and CHANGHUA HU

Department of Urology, Ningbo No. 7 Hospital, Ningbo, Zhejiang 315202, P.R. China

Abstract. Chemotherapy remains one of the most important adjuvant treatments for bladder cancer (BC). However, similar to other malignancies, BC is prone to chemotherapy resistance and only approximately half of muscle-invasive patients with BC respond to chemotherapy. The present study aimed to reveal the mechanisms underlying chemoresistance in BC cells. Cell viabilities were assessed by CCK-8 assay. The differentiated expression of genes in chemoresistant and their parental BC cells were examined by RNA sequencing. Cell death was determined by flow cytometry. Different cell death inhibitors were used to determine the types of cell death. Levels of reactive oxygen species, iron, glutathione and malondialdehyde were assessed using the corresponding commercial kits. ChIP and dual luciferase activity assays were performed to investigate the interaction between staphylococcal nuclease and tumour domain containing 1 (SND1) and glutathione peroxidase 4 (GPX4) mRNA. RNAi was used to knockdown SND1 or GPX4. The results revealed that SND1 in BC cells were insensitive to cisplatin, and inhibition of SND1 overcame this resistance. Silencing of SND1 enhanced cell death induced by cisplatin by promoting ferroptosis in BC cells. Mechanistically, SND1 was revealed to bind to the 3'UTR region of GPX4 mRNA and stabilise it. Knockdown of GPX4 could also overcome chemoresistance, and overexpressing GPX4 reversed the effects of silencing of GPX4 on the chemosensitivity of BC cells. Thus, targeting the SND1-GPX4 axis may be a potential strategy to overcome chemoresistance in BC cells.

Introduction

Bladder cancer (BC) is one of the most common malignancies of the urinary tract, accounting for over 70,000 new cases and 16,000 cancer-related deaths in the USA each year (1). Furthermore, based on the formation pathway, BC can be divided into two groups: Non-muscle-invasive BC and muscle-invasive BC (2). Currently, radical cystectomy combined with chemotherapy is the mainstream treatment for muscle-invasive BC. However, patients with BC often respond poorly to standard chemotherapeutic agents (3). Thus, it is necessary to identify the mechanisms underlying chemoresistance in BC.

Ferroptosis is a novel form of cell death that is featured by iron-dependent peroxidation of the lipid membrane induced by the accumulation of massive amounts of reactive oxygen species (ROS) (4). Glutathione peroxidase 4 (GPX4) is an antioxidant that can reduce peroxide, such as hydrogen peroxide and organic hydroperoxides, by cooperating with the antioxidant glutathione (GSH) (5). Therefore, during the process of ferroptosis, inhibition of GPX4 is one of the key events (5). Since ferroptosis is biochemically different from other forms of cell death, induction of ferroptosis may be a promising strategy for overcoming chemoresistance in various cancer cells.

Staphylococcal nuclease and tudor domain containing 1 (SND1) is recognized as a novel oncoprotein that is upregulated in numerous types of cancer cells (6). SND1 was identified as a transcription factor that is involved in diverse post-transcriptional regulation activities, such as mRNA splicing, RNA stability and editing (7). Furthermore, SND1 is ubiquitously expressed and highly conserved in mammals and plays essential physiological roles in various biological activities, such as cell proliferation, differentiation and death (6). SND1 has also been revealed to be correlated with chemoresistance to cisplatin in non-small cell lung cancer (NSCLC) cells (8). At present, there is little knowledge concerning the role of SND1 in BC.

The present study aimed to identify the factors that contribute to the resistance of cisplatin in BC cells. The results demonstrated that the inhibition of SND1 could overcome chemoresistance in BC cells by promoting ferroptosis. Mechanistically, SND1 was revealed to bind to the 3'UTR region of GPX4 mRNA and stabilise it. The findings of the present study suggest that targeting SND1 may be a promising strategy to overcome chemoresistance in BC.

Materials and methods

Cell culture and chemicals. Human bladder cancer cells T24 (ATTC no. HTB-4), 5637 (ATTC no. HTB-9) and RT-4

Correspondence to: Dr Changhua Hu, Department of Urology, Ningbo No. 7 Hospital, 718 Nan Er Xi Road, Ningbo, Zhejiang 315202, P.R. China
E-mail: huchanghuaurology@163.com

(ATTC no. HTB-2) were obtained from American Type Culture Collection (ATCC). RT-112 (product no. 300324) and CLS-439 (product no. 300150) were obtained from Cell Lines Service GmbH. The cisplatin-resistant T24/R and 5637/R cells were created by stepwise escalation method: Parental T24 and 5637 cells were cultured with gradually increasing concentrations of cisplatin from 2 nM to 1 μM over 8 months. All cells were cultured in RPMI-1640 medium supplemented with 10% fetal bovine serum (FBS) and 1% penicillin and streptomycin in humidified air with 5% CO_2 at 37°C. All cells were authenticated by STR profiling and tested for *Mycoplasma* contamination by Shanghai Biowing Applied Biotechnology Co., Ltd. The following reagents were used in the present study: Pan-capase inhibitor [Z-VAD-FMK (z-VAD); cat. no. S7023; Selleck Chemicals], necrostatin-1 (Nec-1; cat. no. S8037; Selleck Chemicals), Liproxstatin-1 (Lip-1; product no. 950455-15-9; Sigma-Aldrich; Merck KGaA), ferrostatin-1 (Fer-1; cat. no. S7243; Selleck Chemicals), deferoxamine (DFO; cat. no. HY-B0988; MedChemExpress), L-γ-glutamyl-p-nitroanilide (GPNA; cat. no. S6670; Selleck Chemicals), N-acetylcysteine (cat. no. S1623; Selleck Chemicals), actinomycin D (ActD; cat. no. S8964; Selleck Chemicals). The concentrations of the various inhibitors used were as follows: z-VAD, 20 mM; Nec-1, 10 mM; Lip-1, 10 mM; Fer-1, 10 mM; DFO, 10 mM; and GPNA, 10 mM. The inhibitors were added into the culture medium and incubated with cells at 37°C. Cisplatin (product no. 15663-27-1) and all other routine chemicals were purchased from Sigma-Aldrich; Merck KGaA.

Assessment of ROS. The levels of ROS were assessed using the C11-BODIPY staining kit (cat. no. D3861; Life Technologies; Thermo Fisher Scientific, Inc.) according to the manufacturer's instructions. Briefly, the T24/R and 5637/R cells were seeded into a 24-well plate at a density of 10,000 cells/well. Following various treatments (transfected with shNC/shSND1 or vector/GPX4 OV for 24 h; then treated with or without cisplatin), the cells were collected and stained with C11-BODIPY (5 μM) at 37°C for 0.5 h. The FACSCanto II flow cytometer (BD Biosciences) was used to assess the results. The results were analyzed using the FlowJo 2.0 software (Tree Star, Inc.).

Assessment of cell death. T24/R and 5637/R cells were seeded onto a 6-well plate at a density of $1x10^6$ cells/well. Following various treatments (transfected with shNC/shSND1 or vector/GPX4 OV for 24 h; then treated with or without cisplatin), cells were collected and resuspended with PBS and stained with Annexin V-fluorescein isothiocyanate (FITC)/propidium iodide (PI) solution (BD Biosciences) at room temperature for 30 min. The Annexin V-FITC/PI positive cells were analysed by flow cytometry on BD FACSCalibur (BD Biosciences). The results were analyzed using the FlowJo 2.0 software.

Assessment of ferrous ions (Fe2+), GSH and lipid peroxidation marker, malondialdehyde (MDA). The levels of Fe2+, GSH and MDA were assessed using the Iron Assay Kit (product code ab83366, colorimetric), GSH assay kit (product code ab239727, colorimetric) and MDA assay kit (product code ab118970, colorimetric), according to the manufacturer's guide respectively. All kits were obtained from Abcam.

Reverse transcription-quantitative polymerase chain reaction (RT-qPCR). Total RNA was extracted from the cells using TRIzol reagent (Beijing Solarbio Science & Technology Co., Ltd.) according to the manufacturer's instructions. The mRNA levels of various genes were assessed using a first-strand cDNA synthesis kit (cat. no. K1612) and SYBR Green Master Mix kit (cat. no. A25741; both from Thermo Fisher Scientific, Inc.) according to the manufacturer's instructions. The quantitative real-time PCR reaction was performed using an ABI 7500 Fast real-time PCR system (Applied Biosystems; Thermo Fisher Scientific, Inc.). The following thermocycling conditions were used: Initial denaturation at 95°C for 10 min followed by 35 cycles at 95°C for 15 sec, 55°C for 30 sec, 72°C for 30 sec and a final extension at 72°C for 5 min. The expression of glyceraldehyde 3-phosphate dehydrogenase (GAPDH) was used as an internal control. The following primers were used in the present study: SND1 forward, 5'-GTGGACAGC GTAGTTCGGGA-3' and reverse, 5'-CCCACGAGACATTTC CACACAC-3'; SLC7A11 forward, 5'-GGGCAGCGTGGG CATGTCTCT-3' and reverse 5'-GGACCAAAGACTTCC AAAATA-3'; ACSL4 forward, 5'-GCCCACTTCAGACAA ACCTGG-3' and reverse, 5'-ACAGCTTCTCTGCCAAGT GTGG-3'; SLC3A1 forward, 5'-GGGTGTTGATGGTTTTAG TTTGGAT-3' and reverse, 5'-GCATTCCCACCTGCGAGG TGGAGAAG-3'; GPX4 forward, 5'-GGGACGACTGGCGCT GTGCGCGCTCC-3' and reverse, 5'-CTCACTGGGAGGCCA CGTTG-3'; GSS forward, 5'-CTTCAACCTGCTAGTGGA TGCTGT-3' and reverse, 5'-TGGAACATGTAGTCTGAG CGATTC-3'; GCL forward, 5'-TTGCCTCCTGCTGTGTGA TG-3' and reverse, 5'-ATCATTGTGAGTCAACAGCTGTAT GTC-3'; GAPDH forward, 5'-TGAAGGTCGGAGTCAACG GATTTGGT-3' and reverse, 5'-CATGTGGGCCATGAGGTC CACCAC-3'. The gene expression levels were calculated using the $2^{-\Delta\Delta Cq}$ method (9).

Luciferase assay. The wild-type and truncated mutant 3'UTR of GPX4 were inserted into the pGL3-basic vector (Life Technologies; Thermo Fisher Scientific, Inc.). The empty vector (EV) and SND1 expressing vector (SND1 OV) and pGL3 vector were co-transfected into the cells using Lipofectamine 2000 reagent (Life Technologies; Thermo Fisher Scientific, Inc.) according to the manufacturer's instructions. The cells were collected 48 h after transfection and then assayed by the Dual-luciferase reporter assay system (Promega Corporation). The relative firefly activity was normalized to *Renilla* luciferase activity according to the manufacturer's instructions.

Chromatin IP (ChIP) analysis. ChIP analysis was carried out using a Millipore EZ-Magna ChIP kit (cat. no. 17-295; EMD Millipore) according to the manufacturer's protocol. Briefly, the T24/R and 5637/R cells were seeded into a 6-well plate at a density of $5x10^6$ cells/well. The cells were collected after 24 h of treatment and fixed with 1% formaldehyde for 10 min at room temperature. After rehydrating in 0.125 M glycine, the cells were washed in phosphate-buffered saline (PBS) and resuspended in ChIP lysis buffer. The cell lysate was centrifuged at 10,000 x g for 10 min at 4°C. Anti-immunoglobulin G (IgG) (product code ab131368; Abcam) or anti-SND1 antibody (product code ab65078; Abcam) were incubated with Dynabeads protein G (cat. no. 10003D; Life Technologies;

Thermo Fisher Scientific, Inc.) for 2 h at 4˚C, followed by incubation with precleared chromatin overnight at 4˚C. The precipitated RNA samples and inputs were subjected to RT-qPCR.

Short hairpin RNA (shRNA) transfection. shRNA against SND1 (shSND1#1, 5'-AAGGCATGAGAGCTAATAATC-3'; and shSND1#2, 5'-GCCACAACCAGAACATTCTG-3'); GPX4 (shGPX4#1, 5'-CATCGTCACCAACGTGGCC-3'; and shGPX4#2 5'-TCAAATTCGATATGTTCAGCAAGA-3') and negative control shRNA (shNC; 5'-CCATCGCATTCACTATGCTAAG-3') were purchased from Shanghai GenePharm Co., Ltd.

shRNAs were subcloned into the pSilencer 4.1-CMV FANCF shRNA vector (Life Technologies; Thermo Fisher Scientific, Inc.). The transfection was performed using Lipofectamine 2000 (Life Technologies; Thermo Fisher Scientific, Inc.) according to the manufacturer's guide. Briefly, the T24/R and 5637/R cells were seeded into 6-well plates at a density of 2.5×10^6 cells/well in full RPMI-1640 medium. When the cells reached ~70% confluence, the culture medium was replaced with 2 ml fresh complete medium. A total of 2.5 μg of plasmid was then diluted in 100 μl of Opti-MEM medium (Life Technologies; Thermo Fisher Scientific, Inc.) with 5 μl of Lipofectamine 2000. The solution was incubated at room temperature for 30 min and added into the cells. Subsequently, 24 h later, western blotting was used to assess the efficiency of the transfection.

Overexpression of SND1 and GPX4. To overexpressing SND1 and GPX4, full-length cDNAs were subcloned into pcDNA3.1 vector (Life Technologies; Thermo Fisher Scientific, Inc.) and a blank vector was used as a negative control. Vectors were transfected into cells using Lipofectamine 2000 (Life Technologies; Thermo Fisher Scientific, Inc.) according to the manufacturer's instructions. Briefly, 10 μg of plasmids were diluted into 250 μl Opti-MEM medium (Life Technologies; Thermo Fisher Scientific, Inc.), and gently mixed at room temperature for 5 min. Subsequently, 5 μl of Lipofectamine 2000 was added into the mixed Opti-MEM medium and incubated at room temperature for 20 min. The Opti-MEM medium was added into cells and supplemented with 750 μl of RPMI-1640 medium. A total of 6 h later, the medium was changed with fresh RPMI-1640 medium. The transfection efficiency was evaluated 48 h later using western blotting.

Western blotting. Cells were lysed using the radioimmunoprecipitation assay (RIPA) buffer (Beyotime Institute of Biotechnology), and the Bradford assay kit was used to measure the protein concentrations. An equal amount of protein (20 μg) was resolved on a 10% SDS-polyacrylamide gel electrophoresis (PAGE) and transferred to a polyvinylidene fluoride (PVDF; BD Biosciences) membrane. The PVDF membranes were then blocked with 5% skimmed milk at room temperature for 1 h. Subsequently, the membranes were incubated with primary antibodies at following dilutions: Caspase-3 (product no. 14220; dilution 1:1,000; Cell Signaling Technology, Inc.), SND1 (product code ab65078; dilution 1:1,000; Abcam), GPX4 (product no. 52455; dilution 1:1,000; Cell Signaling Technology, Inc.), GAPDH (product no. HPA040067;

1:10,000; Sigma-Aldrich; Merck KGaA) overnight at 4˚C. The membranes were then incubated with secondary horseradish peroxidase-conjugated antibodies (sheep-anti-rabbit; product no. AP510; 1:5,000; Sigma-Aldrich; Merck KGaA). The results were visualized using the Chemiluminescent Imaging System (Tanon Science and Technology Co., Ltd.).

RNA sequencing (RNA-seq). The total cellular RNA was extracted using TRIzol (cat. no. 15596018; Life Technologies; Thermo Fisher Scientific, Inc.) according to the manufacturer's instructions. NanoDrop 2000 spectrophotometer (Thermo Fisher Scientific, Inc.) was used to determine the quality of RNA. The RNA samples that met the following criteria were used in the following investigations: RNA integrity number >7.0 and 28S:18S ratio >1.5. Messenger RNA templates were then isolated with oligo-dT Dynabeads (cat. no. 61005; Thermo Fisher Scientific, Inc.) according to the manufacturer's instructions and fragmented to an average size of 200 nucleotides by incubation in fragmentation buffer (cat. no. B0330, Enzymatics; Qiagen, Inc.) for 2 min at 70˚C. Sequencing libraries and data analysis were constructed and performed by BioMarker Technologies Corporation. Briefly, mRNA sequencing libraries were created using the Illumina TruSeq Stranded mRNA library Prep Kit (cat. no. RS-122-2101; Illumina, Inc.) according to the manufacturer's instructions. The quality of the libraries was verified using Caliper LabChip GX/HT DNA High sensitivity Kit (cat. no. 50674626; PerkinElmer Inc.). The quantitation of libraries was verified by Qubit dsDNA HS (cat. no. Q32851; Thermo Fisher Scientific, Inc.). The paired-end sequencing was performed using the NovaSeq 6000 sequencing system (Illumina, Inc.) with a final library concentration of 6 pM as determined by qPCR. The heat map was designed to visualize the results using ggplots v3.0 (https://cran.r-project.org/web/packages/ggsignif/ggsignif.pdf), which is a package based on the R language. RNA sequencing data was uploaded at NCBI Sequence Read Archive (SRA) database (accession no. PRJNA835161; https://www.ncbi.nlm.nih.gov/bioproject/PRJNA835161).

Enrichment analysis using kyoto encyclopedia of genes and genomes (KEGG). KEGG pathway analysis (10) was conducted to analyze the overlapping differentially expressed genes (DEGs). KEGG pathway analysis revealed biological pathways associated with DEGs. A P-value <0.05 was used as the cutoff standard.

Statistical analysis. All statistical analyses were performed using SPSS12.0 (SPSS, Inc.). Data are presented as the mean ± standard error. All experiments were repeated at least three times. Statistical differences between two groups were determined using the unpaired Student's t-test or one-way analysis of variance followed by post hoc Tukey's test for multiple comparisons. P<0.05 was considered to indicate a statistically significant difference.

Results

SND1 regulates the sensitivity of BC cells to cisplatin. First, the IC_{50} values of the response of different BC cells to cisplatin
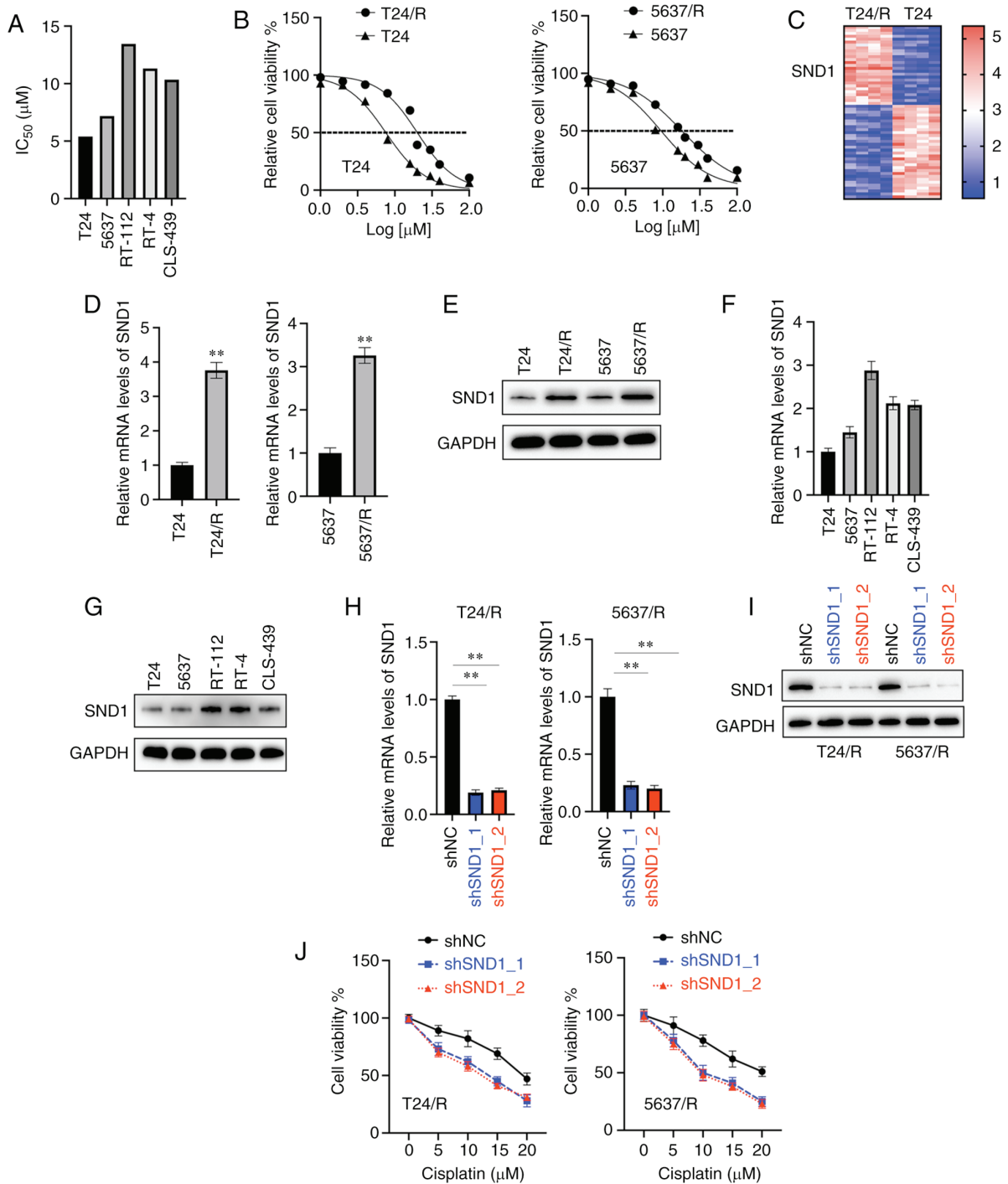
Figure 1. Silencing of SND1 increases the sensitivity of BC cells to cisplatin. (A) The IC$_{50}$ values of the response of BC cells to cisplatin. (B) Treatment of T24/R, T24, 5637/R and 5637 cells with various concentrations of cisplatin for 24 h, and assessment of their cellular viabilities. (C) RNA sequencing analysis of gene expression in T24/R and T24 cells. (D) mRNA levels of SND1 were assessed by reverse transcription-quantitative polymerase chain reaction in T24, T24/R, 5637 and 5637/R cells. (E) Western blotting was used to assess the protein levels of SND1. (F) mRNA levels of SND1 in various BC cells. (G) Protein levels of SND1 in various BC cells. (H) T24/R and 5637/R cells were transfected as indicated, and the mRNA levels of SND1 were assessed. (I) T24/R and 5637/R cells were transfected as indicated, and protein levels of SND1 were determined. (J) T24/R and 5637/R cells were transfected as indicated, and treated with various concentrations of cisplatin for 24 h, and their cellular viabilities were assessed. Data are presented as the mean ± standard deviation. **P<0.01. SND1, staphylococcal nuclease and tudor domain containing 1; BC, bladder cancer; sh, short hairpin RNA; NC, negative control.

were determined (Fig. 1A). Because T24 and 5637 cells were more sensitive than other BC cells, they were selected to create cisplatin-insensitive BC cells. Cell viability assays revealed that T24/R and 5637/R cells were markedly less sensitive to cisplatin than the parental T24 and 5637 cells (Fig. 1B). To reveal the potential mechanisms underlying the resistance

to cisplatin in BC cells, RNA seq was conducted in T24 and T24/R cells. It was determined that SND1 was significantly upregulated in T24/R cells compared with T24 cells (Fig. 1C). RT-qPCR confirmed that SND1 mRNA was significantly increased in T24/R and 5637/R cells compared with T24 and 5637 cells (Fig. 1D). Western blotting also revealed that the

protein levels of SND1 were upregulated in cisplatin-insensitive T24/R and 5637/R cells compared with cisplatin-normal T24 and 5637 cells (Fig. 1E). Furthermore, the expression of SND1 was assessed in various cancer cells. It was found that the mRNA and protein levels of SND1 were negatively associated with the sensitivity to cisplatin in BC cells (Fig. 1F and G). To evaluate whether SND1 could affect the sensitivity of BC cells to cisplatin, two shRNAs were introduced into T24/R and 5637/R cells to knockdown SND1 (Fig. 1H and I). Cell viability assays demonstrated that silencing of SND1 significantly inhibited the cell viability of T24/R and 5637/R cells when treated with cisplatin (Fig. 1J). Collectively, these data indicated that silencing of SND1 overcame resistance to cisplatin in BC cells.

Silencing of SND1 promotes ferroptosis induced by cisplatin in BC cells. Next, it was verified whether silencing of SND1 could affect cell death induced by cisplatin in BC cells. Flow cytometry revealed that knockdown of SND1 significantly promoted cell death caused by cisplatin in T24/R and 5637/R cells (Fig. 2A). To confirm the cell death caused by cisplatin and inhibition of SND1, various cell death inhibitors were applied. Notably, it was found that apoptosis inhibitor (z-VAD) and necrosis inhibitor (Nec-1) had little effect on cell death caused by cisplatin in T24/R and 5637/R cells following knockdown of SND1 (Fig. 2B). In addition, ferroptosis inhibitors Lip-1 and Fer-1 significantly attenuated cell death induced by cisplatin in T24/R and 5637/R cells after knockdown of SND1 (Fig. 2B). To further confirm that the form of cell death was ferroptosis and not any other form, several markers of ferroptosis were used. It was revealed that cisplatin induced a significant increase of Fe^{2+} in T24/R and 5637/R cells after knockdown of SND1 (Fig. 2C), and this effect could be reversed by the iron chelator DFO and glutamine transporter inhibitor GPNA (Fig. 2C). Additionally, cisplatin treatment combined with the knockdown of SND1 induced accumulation of ROS which could be terminated by the ROS scavenger N-acetylcysteine in T24/R and 5637/R cells (Fig. 2D). Assessment of GSH indicated that knockdown of SND1 combined with cisplatin significantly reduced the levels of GSH in T24/R and 5637/R cells (Fig. 2E). In addition, MDA assays showed that the knockdown of SND1 combined with cisplatin significantly promoted the levels of MDA in T24/R and 5637/R cells (Fig. 2F). These findings indicated that knockdown of SND1 overcame the resistance to cisplatin by promoting ferroptosis in cisplatin-resistant BC cells.

SND1 physically binds the 3'UTR of GPX4 mRNA and promotes its stability. To better understand the mechanism of the regulatory effects of SND1 on ferroptosis in BC cells treated with cisplatin, an attempt was made to identify the downstream targets of SND1. According to the KEGG database (http://www.genome.ad.jp/kegg/), several ferroptosis-related genes (*SLC7A11*, *ACSL4*, *SLC3A1*, *GSS*, GPX4 and GCL) were selected as candidates (Fig. 3A). The mRNA levels of the aforementioned candidate genes were assessed after the knockdown of SND1. Compared with the control group (shNC), the relative expression of GPX4 was significantly decreased while other genes were less affected (Fig. 3A). Western blotting also revealed that the protein levels of GPX4 in cisplatin-insensitive

cells were increased compared with their parental cells (Fig. 3B). Knockdown of SND1 also led to the downregulation of GPX4 in T24/R and 5637/R cells (Fig. 3C). SND1 has been reported as a transcription factor that was able to bind with mRNAs (11). It was hypothesized that SND1 may bind with the mRNA of GPX4 and stabilise it. To verify this, first, an RNA immunoprecipitation ChIP assay was performed and high enrichment of GPX4 mRNA in the SND1-RNA binding complex, was determined using anti-IgG as a negative control (Fig. 3D). Furthermore, a vector that successfully overexpressed SND1 (SND1 OV) was constructed in BC cells (Fig. 3E). The sequences of the 5'-UTR, coding sequence (CDS) and 3'-UTR were cloned into the pGL3 vectors and transfected into the BC cells along with EV or SND1 OV to perform dual-luciferase activity assay. It was observed that the overexpression of SND1 markedly increased the relative luciferase activity in BC cells bearing the 3'-UTR but no other sequences (Fig. 3F). To further confirm the interaction between SND1 and the 3'-UTR of GPX4 mRNA, vectors expressing the wild-type 3'UTR (WT) and two truncated mutant forms (Mut 1; Mut 2) were constructed (Fig. 3G). Notably, it was found that SND1 OV increased the luciferase activity in BC cells transfected with the WT and Mut 1 but not the Mut 2 (Fig. 3G). These findings further demonstrated that SND1 binds to the 3'UTR region of GPX4 at the position from nucleotide 765 to nucleotide 865. ActD (2.5 μg/ml) was also used to inhibit the synthesis of new RNAs in either shNC- or shSND1-transfected cells and the mRNA decay at various time-points was assessed. It was determined that ~10 h after ActD treatment, the abundance of GPX4 mRNA was markedly decreased in shSND1-transfected BC cells compared with shNC-transfected cells (Fig. 3H). Collectively these findings indicated that SND1 positively regulated the mRNA stability of GPX4.

Knockdown of GPX4 overcomes chemoresistance of BC cells to cisplatin by promoting ferroptosis. The role of GPX4 in overcoming chemosensitivity in BC cells was investigated. First, two shRNAs were used to knockdown both the mRNA and protein levels of GPX4 in T24/R and 5637/R cells (Fig. 4A and B). As expected, silencing of GPX4 significantly decreased the viabilities of both T24/R and 5637/R cells under the treatment of various concentrations of cisplatin for 24 h (Fig. 4C). Flow cytometric analysis also demonstrated that silencing of GPX4 significantly increased cell death induced by cisplatin in T24/R and 5637/R cells (Fig. 4D). Additionally, it was also observed that silencing of GPX4 led to the significant upregulation of ROS, Fe^{2+} and MDA and downregulation of GSH compared with the shNC group in T24/R and 5637/R cells (Fig. 4E-H). These data indicated that the SND1-GPX4 axis regulated the sensitivity of BC cells to cisplatin and knockdown of GPX4 overcame resistance to cisplatin in BC cells.

Overexpression of GPX4 attenuates ferroptosis caused by cisplatin and knockdown of SND1 in BC cells. Furthermore, the role of the SND1-GPX4 axis in regulating the sensitivity of BC cells to cisplatin was investigated. T24/R and 5637/R cells were transfected with a vector expressing GPX4 that successfully overexpressed the mRNA and protein levels of GPX4 (Fig. 5A and B). Cell viability assays revealed that overexpression of GPX4 significantly promoted cellular
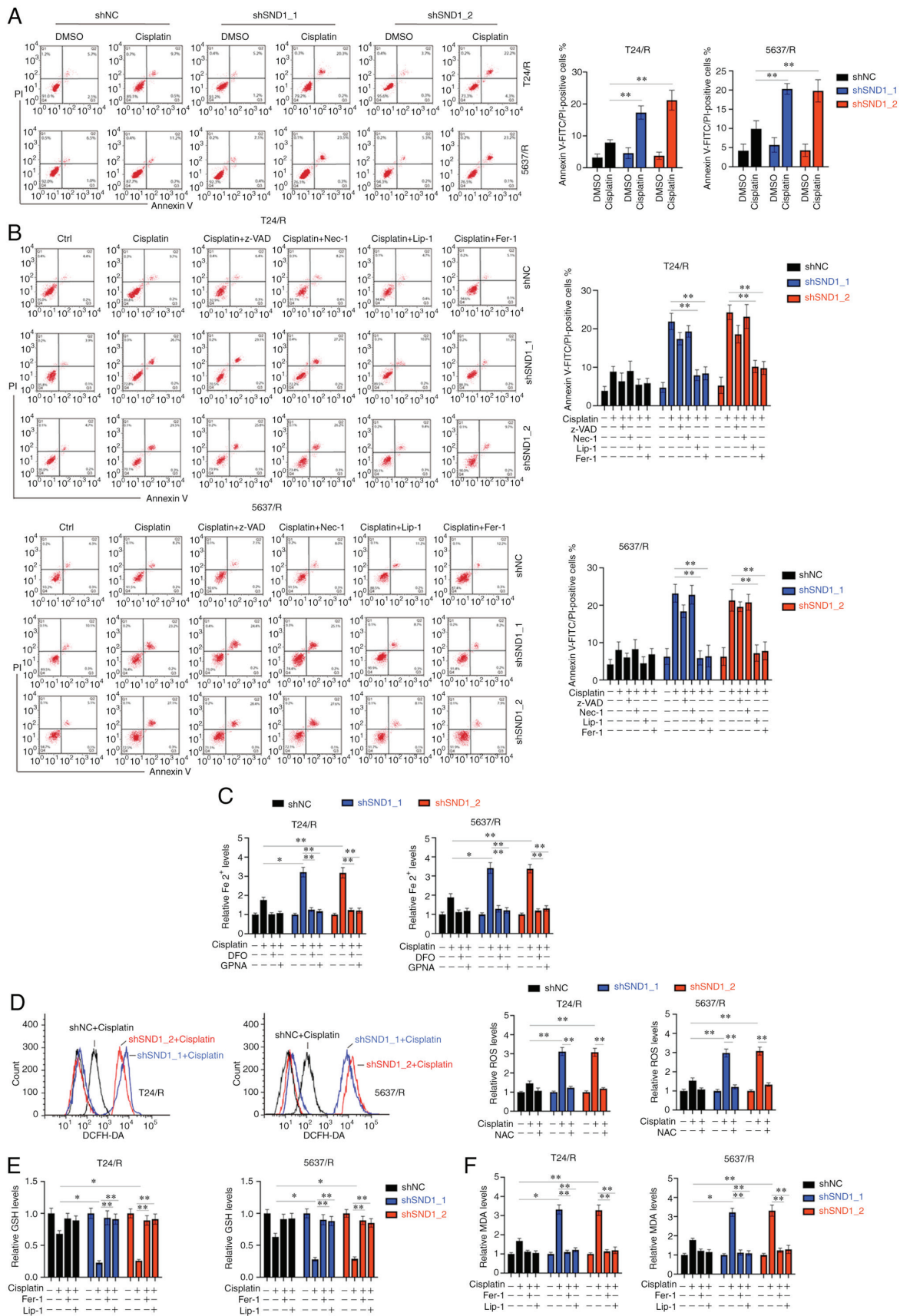
Figure 2. Silencing of SND1 overcomes the resistance to cisplatin by promoting ferroptosis. (A) T24/R and 5637/R cells were transfected as indicated, and treated with or without cisplatin for 24 h, and cellular death was then assessed. (B) T24/R and 5637/R cells were treated as indicated for 24 h, and the cellular death was assessed. (C) T24/R and 5637/R cells were treated as indicated for 24 h, and the iron levels were determined. (D) T24/R and 5637/R cells were treated as indicated for 12 h, and the reactive oxygen species levels were assessed. (E) T24/R and 5637/R cells were treated as indicated for 24 h, and the glutathione levels were determined. (F) T24/R and 5637/R cells were treated as indicated for 24 h, and the MDA levels were assessed. Data are presented as the mean ± standard deviation. *P<0.05 and **P<0.01. SND1, staphylococcal nuclease and tudor domain containing 1; sh, short hairpin RNA; NC, negative control; ROS, reactive oxygen species; GSH, glutathione; MDA, malondialdehyde.
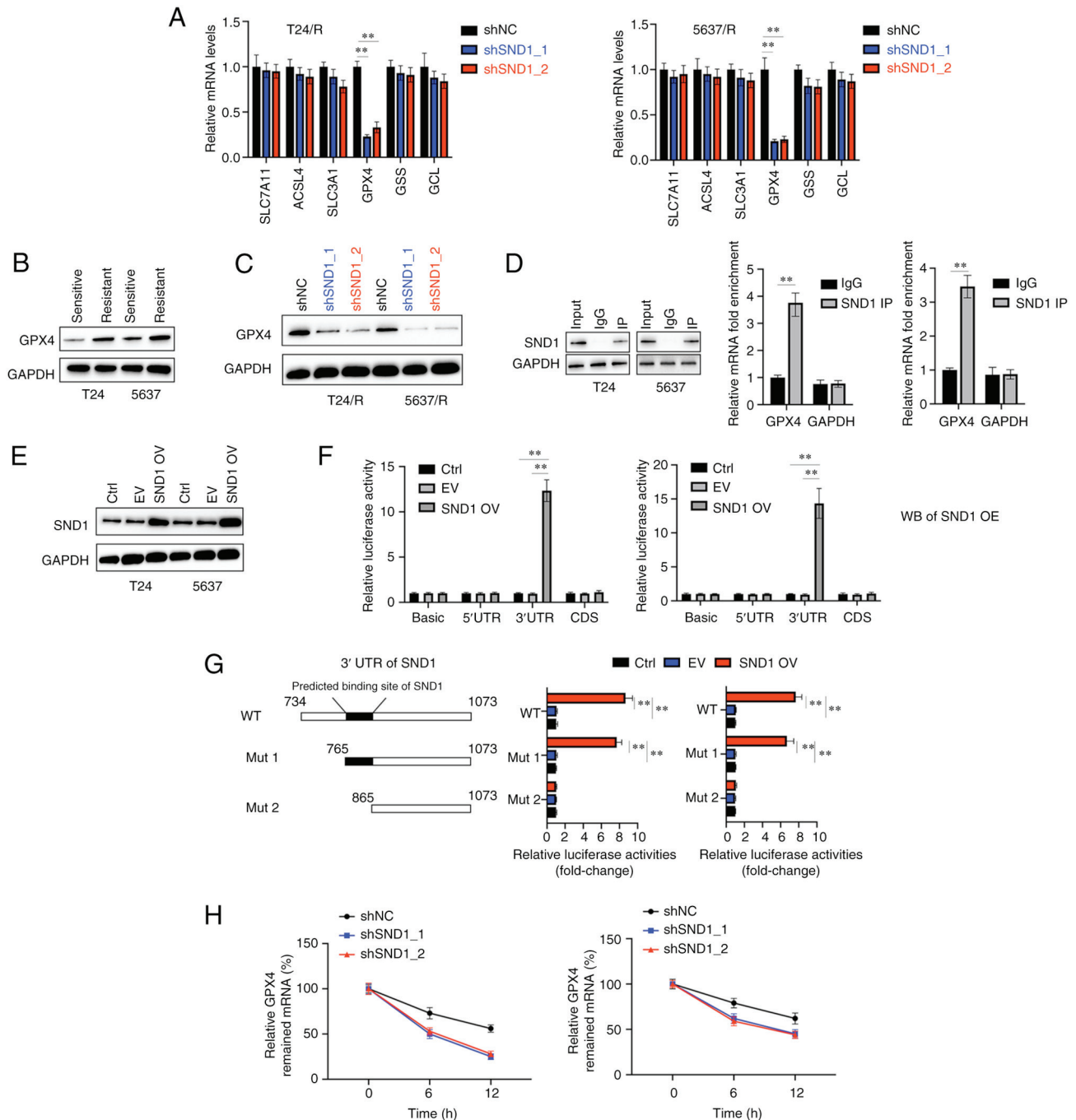
Figure 3. SND1 directly binds to the 3'UTR of GPX4 mRNA and stabilises it. (A) T24/R and 5637/R cells were transfected as indicated, and the mRNA levels of indicated genes were determined. (B) The protein levels of GPX4 were assessed in T24, T24/R, 5637 and 5637/R cells. (C) T24/R and 5637R cells were transfected as indicated, and the protein levels of GPX4 were assessed. (D) T24/R and 5637/R cells were subjected to immunoprecipitation with SND1 antibody or control IgG and GAPDH followed by immunoblotting analysis (left). Reverse transcription-quantitative polymerase chain reaction analysis of the relative enrichment of GPX4 mRNA in SND1-RNA binding complexes, using anti-IgG as a negative control (right). (E) T24 and 5637 cells were transfected as indicated, and the protein levels of SND1 were measured. (F) 5'UTR, 3'UTR and CDS of GPX4 were cloned into a luciferase reporter vector and co-transfected with a vector that expressed SND1 in the T24 and 5637 cells, and the relative luciferase activities were measured. (G) Wild-type or truncated 3'UTR sequences (Mut 1, Mut 2) of GPX4 3'UTR were co-transfected with SND1-expressing vector into T24 and 5637 cells, and the relative luciferase activities were measured. (H) GPX4 mRNA abundance in shNC or shSND1_1 or shSND1_2 transfected cells after actinomycin D (2.5 μg/ml) administration at different time-points (10 and 24 h). Data are presented as the mean ± standard deviation. **P<0.01. SND1, staphylococcal nuclease and tudor domain containing 1; GPX4, glutathione peroxidase 4; CDS, coding sequence; sh, short hairpin RNA; NC, negative control; Ctrl, control; EV, empty vector; OV, overexpression.

viabilities under the treatment of cisplatin and knockdown of SND1 (Fig. 5C). Flow cytometry also indicated that overexpression of GPX4 protected cells from cell death induced by cisplatin and knockdown of SND1 (Fig. 5D). Furthermore, the combined effects of cisplatin and knockdown of SND1 on the

levels of ROS, Fe2+, GSH and MDA could also be abrogated by forced expression of GPX4 in T24/R and 5637/R cells (Fig. 5E-H). These data confirmed that inhibition of SND1 promoted ferroptosis induced by cisplatin and the knockdown of GPX4.
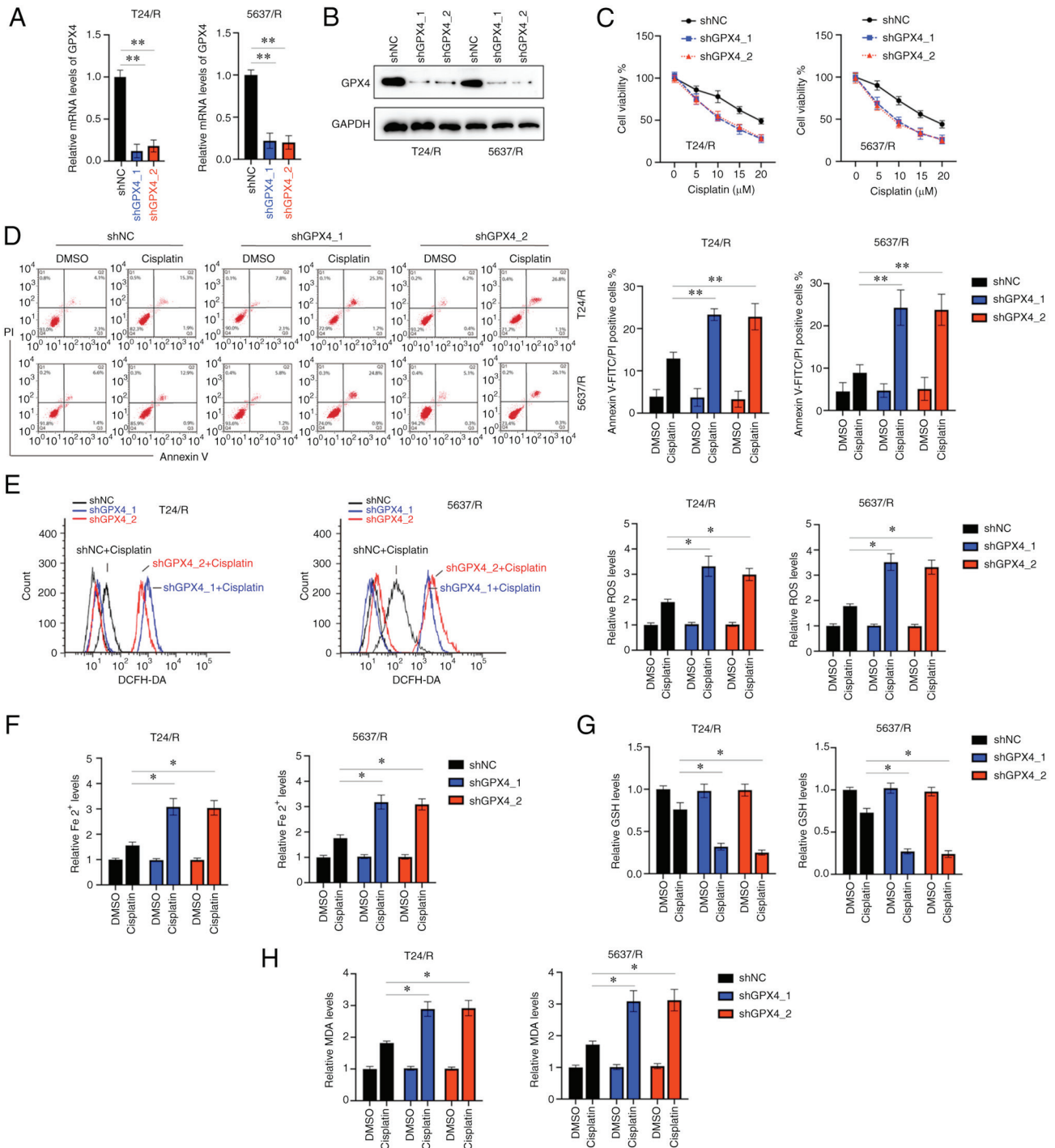
Figure 4. Knockdown of GPX4 overcomes the resistance to cisplatin in BC cells. (A) T24/R and 5637/R cells were transfected as indicated, and the GPX4 mRNA levels were assessed. (B) T24/R and 5637/R cells were transfected as indicated, and the protein levels of GPX4 were determined. (C) T24/R and 5637/R cells were transfected as indicated, and the cells were treated with the indicated concentrations of cisplatin for 24 h, and the cellular viabilities were assessed. (D) T24/R and 5637/R cells were treated as indicated, and cellular death was detected. (E) T24/R and 5637/R cells were treated as indicated, and the reactive oxygen species levels were assessed. (F) T24/R and 5637/R cells were treated as indicated, and the iron levels were determined. (G) T24/R and 5637/R cells were treated as indicated, and the glutathione levels were detected. (H) T24/R and 5637/R cells were treated as indicated, and lipid peroxidation levels were assessed. Data are presented as the mean ± standard deviation. *P<0.05 and **P<0.01. GPX4, glutathione peroxidase 4; BC, bladder cancer; sh, short hairpin RNA; NC, negative control; ROS, reactive oxygen species; GSH, glutathione; MDA, malondialdehyde.

Discussion

Although great progress has been made in the treatment of BC, chemoresistance often hinders the clinical outcomes (12). Furthermore, only half the patients with BC respond to cisplatin-based chemotherapy (13). Recently, evidence has revealed that induction of ferroptosis is a promising strategy to overcome chemoresistance (14). In the present study, it was determined that upregulation of SND1 conferred resistance to cisplatin, whereas knockdown of SND1 overcame resistance to cisplatin by promoting ferroptosis.
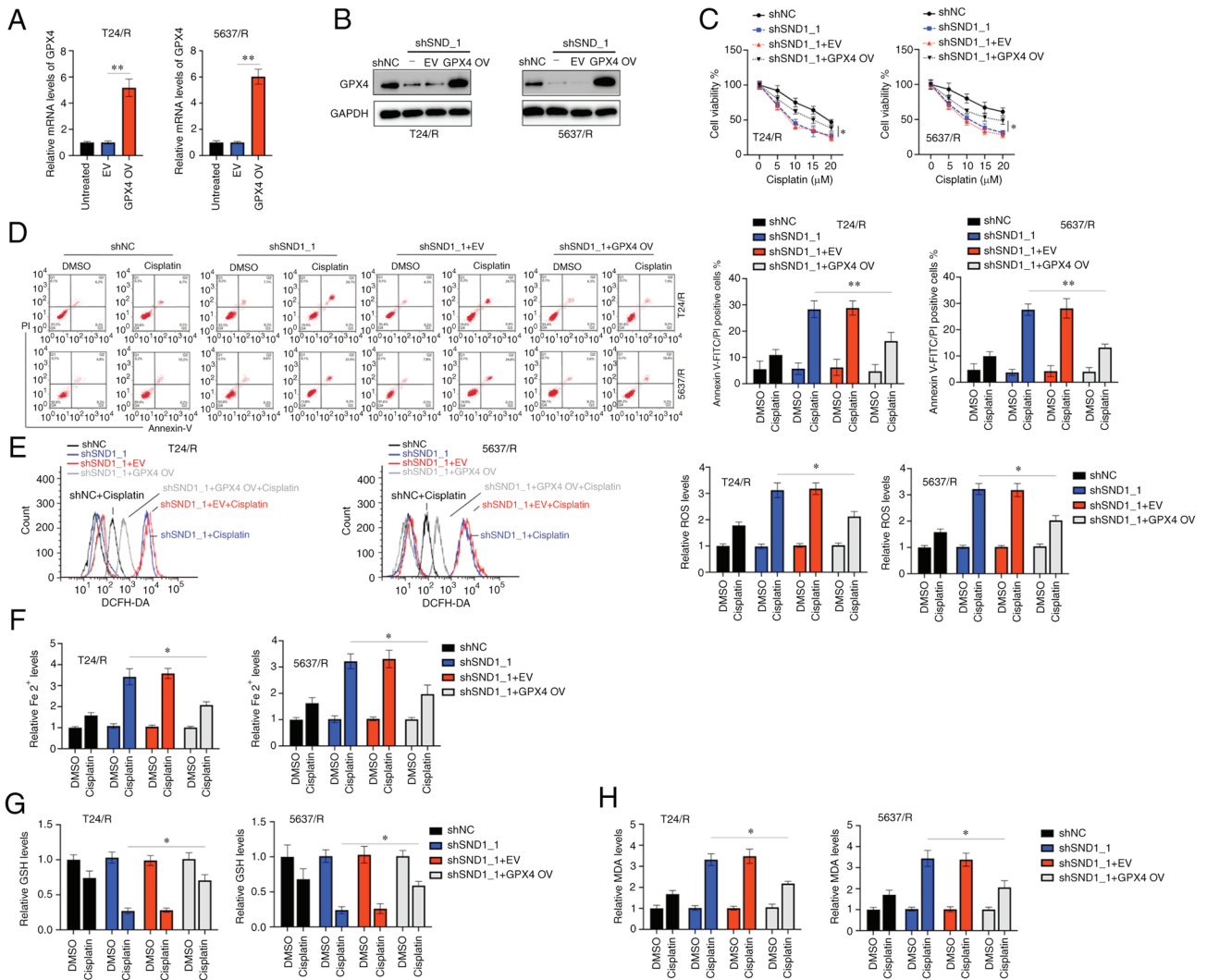
Figure 5. Overexpression of GPX4 reverses the effects of silencing of SND1 on the sensitivity of BC cells to cisplatin. (A) T24/R and 5637/R cells were transfected as indicated for 24 h, and the mRNA levels of GPX4 were determined. (B) The protein levels of GPX4 were assessed. (C) T24/R and 5637/R cells were treated as indicated, and the cellular viabilities were detected. (D) Cellular death was assessed. (E) The reactive oxygen species levels were determined. (F) Th iron levels were detected. (G) The glutathione levels were assessed. (H) Malondialdehyde levels were determined. Data are presented as the mean ± standard deviation. $^*P<0.05$ and $^{**}P<0.01$. GPX4, glutathione peroxidase 4; SND1, staphylococcal nuclease and tudor domain containing 1; BC, bladder cancer; sh, short hairpin RNA; NC, negative control; EV, empty vector; OV, overexpression; ROS, reactive oxygen species; GSH, glutathione; MDA, malondialdehyde.

SND1 gene is located on chromosome 7q31.3 and encodes an evolutionarily conserved protein with five highly conserved domains (15). SND1 was initially identified as a transcription co-factor that interacts with Epstein-Barr nuclear antigen 2 in lymphocytes (16). SND1 has also been reported to be able to form a complex with the splicing factor SAM68 and regulate its splicing activity (11). SND1 has been identified as an oncogene in various cancers such as liver carcinoma, cervical cancer and breast cancer (17-19). However, there is still little knowledge concerning the role of SND1 in BC. A study based on The Cancer Genome Atlas and Gene Expression Omnibus data revealed that high expression of SND1 was correlated with poor prognosis of BC (20). SND1 contributes to the development of cancer through multiple mechanisms, such as transcriptional activation of oncogenes, degradation of tumour suppressor proteins and post-transcriptional inhibition of the mRNA of tumour suppressors (21). SND1 has also been demonstrated to be involved in the chemoresistance of various cancers. For

instance, upregulation of SND1 resulted in blocking of apoptosis and conferring resistance to cisplatin, oxaliplatin and 5-fluorouracil (5-FU) in NSCLC (8). Downregulation of SND1 enhanced apoptosis induced by 5-FU in hepatocellular carcinoma cells (22). In line with the previous studies, the present study also revealed that overexpression of SND1 conferred resistance to cisplatin and inhibition of SND1 overcame this resistance in BC cells. Notably, it was found that SND1 affected cell death caused by cisplatin mainly by regulating ferroptosis and not apoptosis.

Ferroptosis is different from other forms of cell death such as apoptosis, necrosis and autophagy, and has a characteristic accumulation of ROS caused by iron accumulation and lipid peroxidation (4). Strategies to trigger ferroptosis have been demonstrated as a promising anticancer strategy and can mitigate the chemoresistance of tumour cells that escape apoptosis (23). Interestingly, cisplatin-resistant tumour cells are prone to ferroptosis (24). In the present study, it was determined

that cisplatin combined with the silencing of SND1 induced cell death mainly by ferroptosis, as evidenced by the upregulation of ROS, $Fe2^+$, MDA and downregulation of GSH. Mechanistically, it was demonstrated that SND1 positively regulated the expression of GPX4 by binding and stabilising its mRNA. GPX4 belongs to the GPX family and was initially identified to protect liposomes and cellular membranes against iron-catalysed lipid peroxidation (25). Although the role of GPX4 in tumorigenesis is still largely elusive, numerous studies have determined that inhibition of GPX4 can overcome chemoresistance in various cancer cells. For instance, inhibition of GPX4 promoted sensitivity to gefitinib in breast cancer cells (26). Inhibition of GPX4 was also revealed to overcome resistance to various chemotherapeutic agents, such as lapatinib, palbociclib, cisplatin and topotecan in lung cancer cells (27). Another key finding of the present study is that GPX4 mRNA stabilised itself by binding to SND1. Previous studies have revealed that the translation of GPX4 mRNA is under the regulation of various RNA binding proteins, such as guanine-rich sequence-binding factor 1, deleted in azoospermia-associated protein 1 and SECIS binding protein 2 (28-30). Moreover, GPX4 mRNA was also revealed to be directly subjected to the regulation of miRNAs such as miR-214-3p, miR-1224, miR-324-3p and miR-541-3p (31-34). These findings revealed the complexity of the post-transcriptional regulation of GPX4.

Nevertheless, there are still some unresolved issues. First, the upstream events that cause the upregulation of SND1 are still not fully understood. A previous study suggested that nuclear factor-κB, specific protein 1 and nuclear factor Y can act as transcriptional regulators of SND1 (35). Notably, activation of these transcription factors has also been demonstrated to be correlated with the resistance to cisplatin (36). In a future study, it would be of value to assess whether these factors also affect the process of ferroptosis. Second, the findings of the present study were only confirmed in cell lines. It would be of interest to confirm the findings *in vivo*.

In conclusion, the present study indicated that silencing of SND1 overcame the resistance to cisplatin in BC cells by promoting ferroptosis. Mechanistically, investigations revealed that SND1 binds to the 3'UTR of GPX4 and stabilises it. Therefore, targeting the SND1-GPX4 axis may be a potential strategy to overcome chemoresistance in BC cells.

Availability of data and materials

All the data in the present study are available upon reasonable request from the corresponding author.

Authors' contributions

YZ performed most of the experiments. PR repeated the experiments and confirmed the data. ZY performed the statistical analysis. LW repeated some of the experiments and statistical analysis. CH designed the study and drafted the manuscript. YZ and PR confirm the authenticity of all the raw data. All authors read and approved the final manuscript.

Ethics approval and consent to participate

Not applicable.

Patient consent for publication

Not applicable.

Competing interests

The authors declare that they have no competing interests.

References

1. Siegel RL, Miller KD, Fuchs HE and Jemal A: Cancer statistics, 2021. CA Cancer J Clin 71: 7-33, 2021.
2. Sanli O, Dobruch J, Knowles MA, Burger M, Alemozaffar M, Nielsen ME and Lotan Y: Bladder cancer. Nat Rev Dis Primers 3: 17022, 2017.
3. Minato A, Fujimoto N and Kubo T: Squamous differentiation predicts poor response to cisplatin-based chemotherapy and unfavorable prognosis in urothelial carcinoma of the urinary bladder. Clin Genitourin Cancer 15: e1063-e1067, 2017.
4. Dixon SJ, Lemberg KM, Lamprecht MR, Skouta R, Zaitsev EM, Gleason CE, Patel DN, Bauer AJ, Cantley AM, Yang WS, *et al*: Ferroptosis: An iron-dependent form of nonapoptotic cell death. Cell 149: 1060-1072, 2012.
5. Yang WS, SriRamaratnam R, Welsch ME, Shimada K, Skouta R, Viswanathan VS, Cheah JH, Clemons PA, Shamji AF, Clish CB, *et al*: Regulation of ferroptotic cancer cell death by GPX4. Cell 156: 317-331, 2014.
6. Jariwala N, Rajasekaran D, Srivastava J, Gredler R, Akiel MA, Robertson CL, Emdad L, Fisher PB and Sarkar D: Role of the staphylococcal nuclease and tudor domain containing 1 in oncogenesis (review). Int J Oncol 46: 465-473, 2015.
7. Caudy AA, Ketting RF, Hammond SM, Denli AM, Bathoorn AM, Tops BB, Silva JM, Myers MM, Hannon GJ and Plasterk RH: A micrococcal nuclease homologue in RNAi effector complexes. Nature 425: 411-414, 2003.
8. Zagryazhskaya A, Surova O, Akbar NS, Allavena G, Gyuraszova K, Zborovskaya IB, Tchevkina EM and Zhivotovsky B: Tudor staphylococcal nuclease drives chemoresistance of non-small cell lung carcinoma cells by regulating S100A11. Oncotarget 6: 12156-12173, 2015.
9. Livak KJ and Schmittgen TD: Analysis of relative gene expression data using real-time quantitative PCR and the 2(-Delta Delta C(T)) method. Methods 25: 402-408, 2001.
10. Ogata H, Goto S, Sato K, Fujibuchi W, Bono H and Kanehisa M: KEGG: Kyoto encyclopedia of genes and genomes. Nucleic Acids Res 27: 29-34, 1999.
11. Cappellari M, Bielli P, Paronetto MP, Ciccosanti F, Fimia GM, Saarikettu J, Silvennoinen O and Sette C: The transcriptional co-activator SND1 is a novel regulator of alternative splicing in prostate cancer cells. Oncogene 33: 3794-3802, 2014.
12. McKnight JJ, Gray SB, O'Kane HF, Johnston SR and Williamson KE: Apoptosis and chemotherapy for bladder cancer. J Urol 173: 683-690, 2005.
13. Cai Z, Zhang F, Chen W, Zhang J and Li H: miRNAs: A promising target in the chemoresistance of bladder cancer. Onco Targets Ther 12: 11805-11816, 2019.
14. Mou Y, Wang J, Wu J, He D, Zhang C, Duan C and Li B: Ferroptosis, a new form of cell death: Opportunities and challenges in cancer. J Hematol Oncol 12: 34, 2019.
15. Ochoa B, Chico Y and Martinez MJ: Insights into SND1 oncogene promoter regulation. Front Oncol 8: 606, 2018.
16. Tong X, Drapkin R, Yalamanchili R, Mosialos G and Kieff E: The Epstein-Barr virus nuclear protein 2 acidic domain forms a complex with a novel cellular coactivator that can interact with TFIIE. Mol Cell Biol 15: 4735-4744, 1995.

17. Wright T, Wang Y and Bedford MT: The role of the PRMT5-SND1 axis in hepatocellular carcinoma. Epigenomes 5: 2, 2021.
18. Zhan F, Zhong Y, Qin Y, Li L, Wu W and Yao M: SND1 facilitates the invasion and migration of cervical cancer cells by Smurf1-mediated degradation of FOXA2. Exp Cell Res 388: 111809, 2020.
19. Yu L, Liu X, Cui K, Di Y, Xin L, Sun X, Zhang W, Yang X, Wei M, Yao Z and Yang J: SND1 acts downstream of TGFβ1 and upstream of smurf1 to promote breast cancer metastasis. Cancer Res 75: 1275-1286, 2015.
20. Cui X, Zhang X, Liu M, Zhao C, Zhang N, Ren Y, Su C, Zhang W, Sun X, He J, et al: A pan-cancer analysis of the oncogenic role of staphylococcal nuclease domain-containing protein 1 (SND1) in human tumors. Genomics 112: 3958-3967, 2020.
21. Gutierrez-Beltran E, Denisenko TV, Zhivotovsky B and Bozhkov PV: Tudor staphylococcal nuclease: Biochemistry and functions. Cell Death Differ 23: 1739-1748, 2016.
22. Cui X, Zhao C, Yao X, Qian B, Su C, Ren Y, Yao Z, Gao X and Yang J: SND1 acts as an anti-apoptotic factor via regulating the expression of lncRNA UCA1 in hepatocellular carcinoma. RNA Biol 15: 1364-1375, 2018.
23. Hassannia B, Vandenabeele P and Vanden Berghe T: Targeting ferroptosis to iron out cancer. Cancer Cell 35: 830-849, 2019.
24. Guo J, Xu B, Han Q, Zhou H, Xia Y, Gong C, Dai X, Li Z and Wu G: Ferroptosis: A novel anti-tumor action for cisplatin. Cancer Res Treat 50: 445-460, 2018.
25. Shi Z, Zhang L, Zheng J, Sun H and Shao C: Ferroptosis: Biochemistry and biology in cancers. Front Oncol 11: 579286, 2021.
26. Song X, Wang X, Liu Z and Yu Z: Role of GPX4-mediated ferroptosis in the sensitivity of triple negative breast cancer cells to gefitinib. Front Oncol 10: 597434, 2020.
27. Zhang X, Sui S, Wang L, Li H, Zhang L, Xu S and Zheng X: Inhibition of tumor propellant glutathione peroxidase 4 induces ferroptosis in cancer cells and enhances anticancer effect of cisplatin. J Cell Physiol 235: 3425-3437, 2020.
28. Ufer C, Wang CC, Fähling M, Schiebel H, Thiele BJ, Billett EE, Kuhn H and Borchert A: Translational regulation of glutathione peroxidase 4 expression through guanine-rich sequence-binding factor 1 is essential for embryonic brain development. Genes Dev 22: 1838-1850, 2008.
29. Wang Q, Guo Y, Wang W, Liu B, Yang G, Xu Z, Li J and Liu Z: RNA binding protein DAZAP1 promotes HCC progression and regulates ferroptosis by interacting with SLC7A11 mRNA. Exp Cell Res 399: 112453, 2021.
30. Kinzy SA, Caban K and Copeland PR: Characterization of the SECIS binding protein 2 complex required for the co-translational insertion of selenocysteine in mammals. Nucleic Acids Res 33: 5172-5180, 2005.
31. Xie M, Huang P, Wu T, Chen L and Guo R: Inhibition of miR-214-3p protects endothelial cells from ox-LDL-induced damage by targeting GPX4. Biomed Res Int 2021: 9919729, 2021.
32. Li G, Jin J, Liu S, Ding K and Qian C: Inhibition of miR-1224 suppresses hypoxia/reoxygenation-induced oxidative stress and apoptosis in cardiomyocytes through targeting GPX4. Exp Mol Pathol 121: 104645, 2021.
33. Hou Y, Cai S, Yu S and Lin H: Metformin induces ferroptosis by targeting miR-324-3p/GPX4 axis in breast cancer. Acta Biochim Biophys Sin (Shanghai) 53: 333-341, 2021.
34. Xu Q, Zhou L, Yang G, Meng F, Wan Y, Wang L and Zhang L: CircIL4R facilitates the tumorigenesis and inhibits ferroptosis in hepatocellular carcinoma by regulating the miR-541-3p/GPX4 axis. Cell Biol Int 44: 2344-2356, 2020.
35. Armengol S, Arretxe E, Rodriguez L, Ochoa B, Chico Y and Martinez MJ: NF-κB, Sp1 and NF-Y as transcriptional regulators of human SND1 gene. Biochimie 95: 735-742, 2013.
36. Chen HH and Kuo MT: Overcoming platinum drug resistance with copper-lowering agents. Anticancer Res 33: 4157-4161, 2013.